ChemComm
Chemical Communications

Accepted Manuscript

This article can be cited before page numbers have been issued, to do this please use: R. Fukumoto, T. Yokoo, E. Sakuda, K. Omoto, S. Horiuchi, Y. Arikawa and K. Umakoshi, *Chem. Commun.*, 2025, DOI: 10.1039/D5CC03094C.

ROYAL SOCIETY OF CHEMISTRY

rsc.li/chemcomm

ChemComm

View Article Online
DOI: 10.1039/D5CC03094C

COMMUNICATION

Received 00th January 20xx,

Accepted 00th January 20xx

DOI: 10.1039/x0xx00000x

Covalently Linked Triarylborane–Iridium(III) Complex as a Photocatalyst for CO_2 Reduction

Ryo Fukumoto,[a] Takuya Yokoo,[a] Eri Sakuda,*[b] Kenichiro Omoto,[b] Shinnosuke Horiuchi,[c] Yasuhiro Arikawa[b] and Keisuke Umakoshi*[b]

A biscyclometalated Ir(III) complex bearing a triarylborane unit (IrDB) catalyzes the reduction of CO_2 to CO and HCOOH under visible light irradiation in the presence of 1,3-dimethyl-2-phenyl-2,3-dihydro-1*H*-benzo[*d*]imidazole (BIH). A direct covalent linkage between the two components—the Ir(III) metal center and the triarylborane moiety—is essential for achieving the photocatalytic activity.

Carbon dioxide (CO_2) photoreduction is one of the most promising strategies to address global warming and carbon resource depletion and has been the subject of much research over the past decade.[1] Homogeneous CO_2 photoreduction reaction systems typically consist of a catalyst to activate CO_2, a photosensitizer to absorb light, and a sacrificial electron donor. Among these components, metal complexes are often employed as both catalysts and photosensitizers. Ishitani and co-workers, pioneers in this field, have reported highly efficient systems using a variety of complexes with noble metals, including Ru(II),[2] Re(I),[3] Os(II),[4] and Ir(III)[5]. In recent years, there has been a growing interest in replacing these precious metals with more earth-abundant elements, such as base metals[6] and organic molecules[7]. Nevertheless, the use of non-metallic elements as catalytic centers for CO_2 photoreduction is still limited and remains a significant challenge.

Recently, we have developed a series of transition metal complexes in which a triarylborane moiety is connected to an Ir(III)[8] or Ru(II)[9] center and have investigated their unique photophysical properties. These complexes exhibit not only long-lived excited states, but also strong photo absorption in the ultraviolet-visible (UV–vis) region, attributed to π(aryl)–p(B) charge transfer (CT), an intramolecular charge transfer from the metal center or aryl groups to the vacant p orbital of B atom. These characteristics are essential for efficient photosensitizers. Moreover, for the Ru(II) complexes, quenching of photoluminescence was observed in the presence of CO_2 in acetonitrile (MeCN),[9b] suggesting that interaction between CO_2 and the excited state of the complex with the electron density localized on the B atoms. We envisioned that such unique photophysical properties and reactivity toward CO_2 of the metal complexes with triarylborane moiety would render them promising candidates for photocatalysts for the CO_2 photoreduction reaction in which nonmetallic B atom acts as a catalytic center.

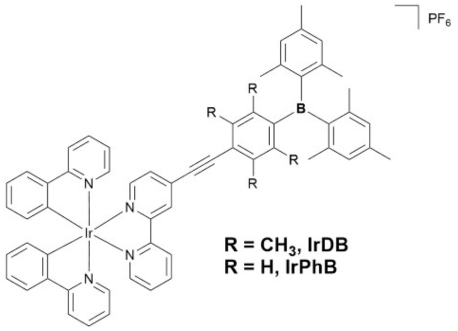

Fig. 1 Chemical structures and abbreviations of Ir(III) complexes.

Herein, we investigated the ability of the Ir(III) complexes bearing a triarylborane moiety as catalysts for CO_2 photoreduction. Unlike Ru(II) complexes, the metal center of the bicyclometalated Ir(III) complexes is generally known to be inactive toward CO_2 activation in photocatalytic systems.[5b]

---

[a] Division of Chemistry and Materials Science, Graduate School of Engineering, Nagasaki University, Bunkyo-machi 1-14, Nagasaki 852-8521, Japan.
[b] Division of Chemistry and Materials Science, Graduate School of Integrated Science and Technology, Nagasaki University, Bunkyo-machi 1-14, Nagasaki 852-8521, Japan. E-mail: sakueri@nagasaki-u.ac.jp
[c] Department of Basic Science, Graduate School of Arts and Sciences, The University of Tokyo, Komaba 3-8-1, Meguro-ku, Tokyo 153-8902, Japan.

† Footnotes relating to the title and/or authors should appear here.

Supplementary Information available: [details of any supplementary information available should be included here]. See DOI: 10.1039/x0xx00000x

View Article Online
DOI: 10.1039/D5CC03084G

Therefore, we focused on Ir(III) complexes (**IrDB** and **IrPhB**, Fig. 1) which possess durylene or phenylene as a linker, respectively (D and Ph refer to durylene and phenylene), to evaluate the photoreactivity of the triarylborane center toward CO_2 photoreduction.

The photophysical properties and chemical reactivities of triarylboranes are known to be strongly influenced by the bulkiness of the surrounding aryls, which affects not only the conformation of the aryl groups and resulting overlap between their π-orbitals and the vacant p-orbital of the B center, but also the accessibility of external molecules to the B center.[10] Focusing on such a structure-properties relationship of the triarylborane derivatives, we designed a new Ir(III) complex (**IrDB**), with a dimesitylboryl moiety connected to the Ir(III) center via a sterically bulky durylene linker in addition to the previously reported **IrPhB**[8a] with a less hindered phenylene linker. The new complex **IrDB** was prepared by a Pd-catalyzed coupling reaction between (ethynylduryl)dimesitylborane and an Ir(III) complex with a bromo-substituted bpy. In addition, reference complexes without triarylborane moiety (**IrD**, Fig. S1) were also prepared and used for a control experiment to discuss the contribution of the triarylborane moiety to the photocatalytic CO_2 reduction. **IrDB** and **IrD** were characterized by ^1H NMR and mass spectrometry (MS) measurements and single-crystal X-ray diffraction (SXRD) analyses (*vide infra*).

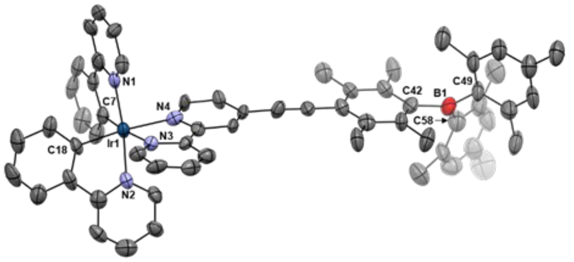

Fig. 2 Crystal structure (ORTEP views at 50% probability level) of **IrDB´**. Solvents, hydrogen atoms, and counter anions (BF_4^-) are omitted for clarity. B: red, C: gray, N: light blue, Ir: dark green.

The SXRD analyses revealed the geometries of the Ir(III) complexes (Fig. 2 for **IrDB´** and Fig. S5 for **IrDB**). Structural analysis of **IrDB** was discussed based on the single crystal structure of a BF_4^- salt (**IrDB´**) since single crystals of the PF_6^- salt suitable for single crystal X-ray diffraction analysis were not obtained despite many attempts at crystallization using various conditions. The Ir–N_{bpy} distances of both complexes were longer than the Ir–N_{ppy} distances owing to the strong σ-donating ability of the C atoms in the cyclometalated ligand (Table S2).[11] Two N atoms in the ppy (ppyH = 2-phenylpyridine) adopt a *trans* configuration. The B atom in **IrDB´** adopts a trigonal planar sp^2-like configuration with B–C distances of 1.56–1.60 Å and C–B–C angles of 119–121° (Table S3). It is notable that the dihedral angle between the BC_3-plane centered on the B atom and the arylene ring is 57° for **IrDB´** (Fig. S6 and Table S3) and 32° for **IrPhB´** (a PF_6^- salt of **IrPhB**),[8a] respectively, suggesting that the π-planes of the durylene moiety of **IrDB´** are rather orthogonal to the BC_3 plane compared to the phenylene moiety of **IrPhB´**. Such a significant difference in the geometries around the B atoms can be explained by the degree of steric repulsion between the arylene (i.e., durylene or phenylene) moiety and the mesityl groups surrounding the B atom.

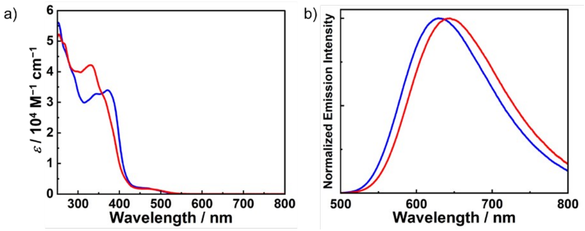

Fig. 3 a) UV–vis absorption spectra and b) emission spectra (λ_{ex} = 420 nm) of Ir(III) complexes in MeCN at 298 K (**IrDB**: blue solid curve, **IrPhB**[7a]: red solid curve).

Fig. 3a shows the absorption spectra and emission spectra of **IrDB** and **IrPhB**[8a] in MeCN at 298 K respectively, with their photophysical parameters summarized in Table S4. Both Ir(III) complexes show a weak absorption band between 450 and 500 nm attributed to metal-to-ligand CT (MLCT). In addition, they exhibit an intense absorption band in 300–400 nm with maximum molar extinction coefficients (ε) of which were 3.39×10^4 M^{-1} cm^{-1} at 373 nm for **IrDB** and 4.22×10^4 M^{-1} cm^{-1} at 332 nm for **IrPhB**, respectively. The spectral comparison between **IrDB** and **IrD** (Fig. S1) is presented in Fig. S7. The ε value of **IrDB** in 300–400 nm is larger than that of **IrD**. Such similarity to **IrPhB** and differences to **IrD** indicate that the absorption of **IrDB** in 300–400 nm originates from the CT transitions involving the triarylborane moiety.[8] The absorption bands in $\lambda > 400$ nm of **IrDB** are assigned to MLCT (Ir center → triarylborane-ethynylene-bpy ligand) and ligand-to-ligand CT (LLCT; ppy → triarylborane-ethynylene-bpy ligand) (S_0–S_1 transition) by time-dependent density functional theory (TD-DFT) calculation (Fig. S8–S9 and Table S5).

The emission maxima of **IrDB** (λ_{ex} = 628 nm) located at a shorter wavelength region than that of **IrPhB** (λ_{ex} = 644 nm) as shown Fig. 3b. This result is in good agreement with the difference in their highest occupied molecular orbital (HOMO)–lowest unoccupied molecular orbital (LUMO) gaps evaluated based on TD-DFT calculation (Fig. S10). Other photophysical properties—the emission quantum yields (Φ_{em}), the emission lifetime (τ_{em}), the radiative (k_r) and nonradiative decay rate constants (k_{nr})—, of **IrDB** and **IrPhB** are nearly comparable (Table S4). This result suggests that the excited state energies and lifetimes of these complexes are not significantly altered by the bridging aromatic ring.

Photocatalytic CO_2 reduction reactions were carried out by photoirradiation ($\lambda_{ex} > 400$ nm) of the MeCN/triethanolamine (TEOA) (5/1 v/v) mixed solutions containing **IrDB** or **IrPhB** (0.05 mM) as photocatalysts and BIH (0.1 M) as the electron donor (ED) under a CO_2 atmosphere. In the cases of both complexes, the evolutions of HCOOH and CO were detected accompanied by the evolution of H_2 (Fig. 4 and Entries 1 and 2 in Table 1). The turnover number (TON) of **IrDB** reached 44 for CO and 36 for HCOOH at 72 h, suggesting that **IrDB** exhibited high stability as a photocatalyst for CO_2 reduction. On the other hand, the TON values for CO and HCOOH with **IrPhB** were lower (TON_{CO} = 2 and TON_{HCOOH} = 11). It is notable that H_2 evolution significantly proceeded in both cases under this reaction condition, indicating that H_2 evolution is one of the major competing pathways with CO_2 photoreduction. In reaction using **IrDB**, CO and HCOOH were scarcely formed in the absence of BIH, TEOA, or light, indicating that all three are essential for the photocatalytic CO_2 reduction (Entries 3–5 in Table1). The origin of CO and HCOOH in the photocatalytic reaction with **IrDB** was confirmed to be CO_2 based on $^{13}CO_2$-labeling experiments. GC-MS analysis of the gas phase after the reaction showed predominant formation of ^{13}CO (m/z = 29), with minimal ^{12}CO detected (Fig. S18). Likewise, the ^1H NMR spectrum of the solution after the reaction showed a clear signal for $H^{13}COOH$, while $H^{12}COOH$ was scarcely observed (Fig. S19).

Table 1. The results of photocatalytic CO_2 reduction for 72h.[a]

Entry	Photocatalyst	TON		
		CO	HCOOH	H_2
1	**IrDB**[b]	44	36	3321
2	**IrPhB**[b]	2	11	590
3	**IrDB**[c]	-	7	46
4	**IrDB**[d]	2	5	50
5	**IrDB**[e]	-	-	-
6	**IrD**[b]	-	8	696
7	**Irbpy**[b]	-	2	301
8	**Irbpy + BDE**[f]	-	6	80
9	**BDE**[g]	-	-	-

[a] The maximum TONs of CO, HCOOH and H_2. Reaction conditions: CO_2-saturated MeCN/TEOA (5/1 v/v, 3 mL) solutions containing photocatalyst and BIH (0.1 M) were irradiated at λ_{em} > 400 nm (Supplementary Information). [b] The concentration of each Ir(III) complex was 0.05 mM. [c] In the absence of BIH. [d] In the absence of TEOA. [e] Under dark. [f] The concentrations of **Irbpy** and (4-ethynyl-2,3,5,6-tetramethylphenyl)bis(2,4,6-trimethylphenyl)borane (**BDE**) were 0.05 mM and 0.05 mM, respectively. [g] The concentration of **BDE** was 0.05 mM.

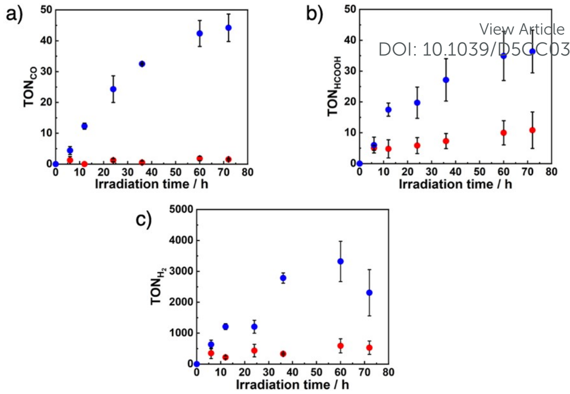

Fig. 4 Photocatalytic production of a) CO, b) HCOOH and c) H_2 as a function of irradiation time using **IrDB** (blue circle, Entry 1 in Table 1) or **IrPhB** (red circle, Entry 2 in Table 1,) as a photocatalyst.

To investigate the difference in the reactivity of the Ir(III) complexes, the reactions of **IrDB** or **IrPhB** with BIH were examined under dark conditions by monitoring the ^1H NMR spectra in CD_3CN (Fig. S11 and S12). In the case of **IrDB**, the signals of **IrDB** remained even after leaving the mixture for 24h. In contrast, the signals of **IrPhB** completely disappeared in the same reaction condition. These results suggest that **IrPhB** reacts with BIH or BI cation[12] produced along with Scheme S1[2c] even under dark conditions, indicating that **IrPhB** does not function as a photocatalyst for CO_2 reduction. It is notable that the reference Ir(III) complexes (**IrD**, **IrPh** and **Irbpy**, Fig. S1) remained intact in the presence of BIH as shown by Fig. S13–S15. This suggests that the dimesitylboryl group connected to the phenylene ring in the Ir(III) complex plays a key structural role leading to the instability of **IrPhB** to BIH or BI cation. The instability of **IrPhB** toward reduction is also supported by cyclic voltammetry (Fig. S20). **IrDB** shows a quasi-reversible redox wave at the cathodic region, whereas **IrPhB** shows a current characteristic of a chemically irreversible process under identical conditions. Although the detailed mechanism remains unclear, the nature of the bridging aromatic ring seems to affect the stability of the Ir(III) complexes with triarylborane or their reduced species. One possible explanation is that the difference in bulkiness between the durylene and phenylene groups attached to the B atom center influences the reactivity of the arylborane moiety. This result underscores the critical role of molecular design in achieving stable and functional photocatalysts.

The emission of **IrDB** was quenched by BIH, as shown by a linear Stern-Volmer plot (Fig. S16). From the slope of the plot ($K_{SV} = 4.07 \times 10^3$ M^{-1}) and emission lifetime (τ_{em}), the quenching rate constant ($k_q = K_{SV}/\tau_{em}$) was calculated to be 1.31×10^{10} $M^{-1}s^{-1}$, which is a sufficient value to realize an efficient photosensitization process.[5] The emission intensity of **IrPhB** also decreased upon addition of BIH, however, the emission maximum of **IrPhB** was slightly shifted implying the possibility of the reaction between **IrPhB** and BIH or BI cation even before photoirradiation as mentioned above (Fig. S16). These results

View Article Online
DOI: 10.1039/D5CC03094C

indicate that only **IrDB** showed the reductive quenching by BIH, generating catalytically active one-electron-reduced species essential for this CO_2 reduction.

To clarify the role of the triarylborane moiety in the photocatalytic CO_2 reduction, control experiments were conducted. Photocatalytic reactions using Ir(III) complexes lacking the dimesitylborane group (**IrD** and **Irbpy**) were performed under the same conditions as those used for **IrDB** (Fig. S1, Entries 6 and 7 in Table 1). In these reactions, H_2 was the major product, along with a small amount of HCOOH (TON_{HCOOH} = 8 for **IrD**, TON_{HCOOH} = 2 for **Irbpy**), while CO formation was not observed. It is known that cyclometalated Ir(III) complexes used as photosensitizers do not function as catalysts for CO_2 reduction even if they undergo partial decomposition during the reaction.[5b] These results indicate that the triarylborane moiety in **IrDB** plays a crucial role as the reaction site for CO formation. Notably, CO was not produced when a mixture of **Irbpy** and **BDE**, or **BDE** alone, were used as catalysts, suggesting that the covalent linkage between Ir(III) complex and the triarylborane moiety via ethynylene linker, which may enable efficient through bond electron transfer, is essential for exhibiting catalytic activity (Fig. S1, Entries 8 and 9 in Table 1). Notably, the presence of TEOA induces significant changes in both the absorption and emission spectra of **IrDB** (Fig. S21), indicating that interactions between **IrDB** and TEOA in the ground and excited states may contribute to the CO_2 photoreduction. Although the mechanism of these interactions remains unclear at this stage, this finding provides an intriguing basis for future studies.

In conclusion, we successfully demonstrated a new photocatalytic system for CO_2 reduction based on a cyclometalated Ir(III) complex bearing a triarylborane moiety. The nature of the arylene linker—either a durylene or a phenylene ring—in the Ir(III) complex significantly influenced the stability of the catalyst in the presence of BIH. **IrDB**, which contains a sterically hindered durylene group, is stable enough to perform CO_2 photoreduction to produce CO and HCOOH, whereas **IrPhB** reacts with BIH or its derivatives even under dark conditions, thereby inhibiting CO_2 photoreduction. Although further optimization and investigation are required, including elucidation of the reaction mechanism and suppression of side reactions such as H_2 evolution, these findings demonstrate potential utilities of the triarylborane moiety to function as a nonmetallic active center for the artificial photosynthesis.

This work was financially supported by JSPS KAKENHI Grant-in-Aid for Transformative Research Areas A (Dynamic exciton, No. 20H05834; E. S.), JST-PRESTO (Grant Number JPMJPR11Q5; E. S.), Tokuyama Science Foundation (E. S.) and the grant from the Nagasaki University (R. F.). The authors thank Dr. Taro Ueda (Nagasaki Univ.) for his support with the GC-MS measurements.

Conflicts of interest

There is no conflict to declare.

Data availability

The data supporting this article have been included as part of the ESI. Crystallographic data have been deposited at the Cambridge Crystallographic Data Centre (CCDC) under deposition number 2365621 for **IrDB´** and can be obtained from https://www.ccdc.cam.ac.uk/structures/.

Notes and references

1 a) B. M. Pirzada, A. H. Dar, M. N. Shaikh, A. Qurashi, *ACS Omega*, 2021, **6**, 29291–29324. b) H. Takeda, C. Cometto, O. Ishitani, M. Robert, *ACS Catal*., 2017, **7**, 70–88.
2 a) K. Kamogawa, A. Santoro, A. M. Cancelliere, Y. Shimoda, K. Miyata, K. Onda, F. Puntoriero, S. Campagna, Y. Tamaki, O. Ishitani, *ACS Catal*., 2023, **13**, 9025–9032. b) A. M. Cancelliere, F. Puntoriero, S. Serroni, S. Campagna, Y. Tamaki, D. Saito, O. Ishitani, *Chem*. Sci., 2020, **11**, 1556–1563. c) Y. Tamaki, K. Tokuda, Y. Yamazaki, D. Saito, Y. Ueda, O. Ishitani, *Front. Chem*., 2019, **7**, 327. d) Y. Yamazaki, A. Umemoto, O. Ishitani, *Inorg. Chem*., 2016, **55**, 11110–11124.
3 a) A. Umemoto, Y. Yamazaki, D. Saito, Y. Tamaki, O. Ishitani, *Bull. Chem. Soc. Jpn*., 2020, **93**, 127–137. b) Y. Tamaki, K. Watanabe, K. Koike, H. Inoue, T. Morimoto, O. Ishitani, *Faraday Discuss*., 2012, **155**, 115–127.
4 a) M. Irikura, Y. Tamaki, O. Ishitani, *Chem. Sci*., 2021, **12**, 13888–13896. b) Y. Tamaki, K. Koike, T. Morimoto, Y. Yamazaki, O. Ishitani, *Inorg. Chem*., 2013, **52**, 11902–11909.
5 a) Y. Kuramochi, O. Ishitani, *Front Chem*., 2019, **7**, 259. b) Y. Kuramochi, O. Ishitani, *Inorg. Chem*., 2016, **55**, 5702–5709.
6 a) Y.-K. Zhang, L. Zhao, W.-J. Xie, H.-R. Li, L.-N. He, *ChemSusChem*, 2024, **17**, e202400090. b) J.-W. Wang, X. Zhang, L. Velasco, M. Karnahl, Z. Li, Z.-M. Luo, Y. Huang, J. Yu, W. Hu, X. Zhang, K. Yamauchi, K. Sakai, D. Moonshiram, G. Ouyang, *JACS Au*, 2023, **3**, 1984–1997. c) J. Shipp, S. Parker, S. Spall, S. L. Peralta-Arriaga, C. C. Robertson, D. Chekulaev, P. Portius, S. Turega, A. Buckley, R. Rothman, J. A. Weinstein, *Inorg. Chem*., 2022, **61**, 13281–13292. d) L.-L. Gracia, L. Luci, C. Bruschi, L. Sambri, P. Weis, O. Fuhr, C. Bizzarri, *Chem. Eur. J*., 2020, **26**, 9929–9937.
7 a) F. Ma, Z.-M. Luo, J.-W. Wang, G. Ouyang, *J. Am. Chem. Soc*., 2024, **146**, 17773–17783. b) P.-Y. Ho, S.-C. Cheng, F. Yu, Y.-Y. Yeung, W.-X. Ni, C.-C. Ko, C.-F. Leung, T.-C. Lau, M. Robert, *ACS Catal*., 2023, **13**, 5979–5985. c) H. Rao, J. Bonin, M. Robert, *ChemSusChem*, 2017, **10**, 4447–4450.
8 a) R. Fukumoto, E. Sakuda, K. Omoto, A. Ito, S. Horiuchi, Y. Arikawa, K. Umakoshi, *Eur. J. Inorg. Chem*., 2025, **28**, e202500054. b) R. Fukumoto, E. Sakuda, K. Omoto, S. Horiuchi, Y. Arikawa, K. Umakoshi, *Chem. Lett*., 2024, **53**, upae237.
9 a) A. Nakagawa, E. Sakuda, A. Ito, N. Kitamura, *Inorg. Chem*., 2015, **54**, 10287–10295. b) E. Sakuda, M. Tanaka, A. Ito, N. Kitamura, *RSC Adv*., 2012, **2**, 1296–1298. c) E. Sakuda, Y. Ando, A. Ito, N. Kitamura, *Inorg. Chem*., 2011, **50**, 1603–1613.
10 a) K. Takaki, E. Sakuda, A. Ito, S. Horiuchi, Y. Arikawa, K. Umakoshi, *RSC Adv*., 2021, **11**, 6259–6267. c) E. Sakuda, A. Funahashi, N. Kitamura, *Inorg. Chem*., 2006, **45**, 10670–10677.
11 a) J.-J. Cao, C.-P. Tan, M.-H. Chen, N. Wu, D.-Y. Yao, X.-G. Liu, L.-N. Ji, Z.-W. Mao, *Chem. Sci*., 2017, **8**, 631–640. b) K. R. Schwartz, R. Chitta, J. N. Bohnsack, D. J. Ceckanowicz, P. Miró, C. J. Cramer, K. R. Mann, *Inorg. Chem*., 2012, **51**, 5082–5094.
12 S. Mehrotra, S. Raje, A. K. Jain, R. Angamuthu, *ACS Sustainable Chem. Eng*., 2017, **5**, 6322–6328.

View Article Online
DOI: 10.1039/D5CC03094C

Data availability

The data supporting this article have been included as part of the ESI. Crystallographic data have been deposited at the Cambridge Crystallographic Data Centre (CCDC) under deposition number 2365621 for **IrDB´**, and can be obtained from https://www.ccdc.cam.ac.uk/structures/.